JOURNAL OF MATERIALS SCIENCE 26 (1991) 1113–1118

Retardation of grain boundary reactions in Ag–Pd–Cu alloys by additions of small amounts of other elements

ISAO KAWASHIMA, YOSHIMA ARAKI, HIROKI OHNO
Department of Dental Materials Science, School of Dentistry, Higashi-Nippon-Gakuen University, Ishikari-Tobetsu, Hokkaido, Japan

The grain-boundary reactions in Ag–25 mass% Pd–10 mass% Cu alloys with 1 mass% aluminium, cobalt, tin, chromium or indium, were investigated by optical microscopy, electrical resistivity, and hardness tests. Addition of tin and chromium retarded grain-boundary reactions. The growth rate of nodules with tin addition was 1/18 of the alloy without additons. Grain-interior reactions are accelerated with chromium, tin and indium addition, with chromium the most effective. The activation energies for the grain-interior and grain-boundary reactions are 192 to 196 and 144 to 208 kJ mol^{-1}, respectively. Additions retard the growth but not the nucleation at the grain boundary. It is concluded that elements which form stable precipitates in the grains retard the grain-boundary reaction.

1. Introduction

Ag–Pd–Cu cast alloys are widely used in dentistry. With age, grain-boundary precipitates ("nodules") are formed in the alloys, resulting in both poorer corrosion resistance and mechanical properties. The nodules are composed of two phases, a silver-rich solid solution (α_2 phase) and a PdCu ordered lattice of the CsCl type (β phase) [1–3].

A previous paper has shown that the internal strain resulting from precipitation in grains is not the driving force for the nucleation of nodules and that the grain-boundary reaction is independent of the stress generated by internal strain [4]. There are many reports of alloy systems where the strain from precipitation in grains becomes the driving force for the formation of the nodules, the grain-boundary reaction for such alloy systems takes place independent of the reaction inside the grains [4]. Therefore, it was hypothesized that the addition of other elements could retard the grain-boundary reactions without obstructing the hardening of the grain interior.

Five elements were selected: low melting point elements (aluminium, tin and indium) considered to accelerate the continuous precipitation, and high melting point elements (cobalt and chromium) considered to retard the grain-boundary reaction due to grain-boundary segregation.

Based on these results, the grain-boundary reactions in Ag–Pd–Cu alloys with additions of 1 mass % of each of these elements were investigated by optical microscopy, electrical resistivity, and hardness tests.

2. Experimental prodedure

Table I shows the elements and the composition (mass %) of the Ag–Pd–Cu alloys used in this study. The alloys contain 64% Ag, 25% Pd, 10% Cu, and 1% additions of aluminium, cobalt, tin, chromium or indium. The alloys were prepared from metals of a purity better than 99.99% in an alumina Tamman tube under an argon atmosphere in a high-frequency induction furnace and then cast in a stainless steel mould; the melted mass of each alloy was 70 g. The weight loss in the melting process was less than 0.02%; chemical analysis after melting was not carried out. The ingots were cold worked slightly and homogenized at 900 °C for 2 h. Block specimens, 5 mm × 5 mm × 10 mm, for optical microscopic observations and hardness measurements, were prepared by cold working as wire specimens, 1 mm × 100 mm, for electric resistivity measurements. For the solution treatment the specimens were kept at 900 °C for several hours before they were quenched in ice–water; then they were heated for different lengths of time to produce a grain size of 120 μm in all the specimens, as nodule formation takes place at the grain boundary. The specimens were aged at 300°, 350°, 400° and 500 °C in a salt bath for 1 to 10^5 min. When ageing was longer than 10^3 min, samples were heated by an electric furnace in a silica tube evacuated by diffusion pump. Electrical resistivity was measured by the four-terminal potentiometric method with a direct current of 20 mA at room temperature.

Hardness tests were performed with a 25 g load by a micro-Vickers hardness tester to distinguish the grain interior from the nodules. The hardness values were averages of ten indentations. Area fraction and nodule widths were measured from several microphotographs (× 400). Identification of phases was made by X-ray diffraction, and concentration profiles of each element were obtained by electron probe micro analysis (EPMA).

0022–2461/90 $03.00 + .12

TABLE I Chemical composition of the alloys

Alloy	Pd	Cu	Ag	Added element (mass %)
1	25	10	65	–
2	25	10	64	Al 1
3				Co 1
4				Sn 1
5				Cr 1
6				In 1

3. Results and discussion

3.1. Optical microstructures

Figs 1 and 2 a to f show the microstructures of alloys 1 to 6 respectively, after solution treatment. Fig. 1a shows the microstructure with equiaxial grains and annealed twins. Fig. 1b shows a second phase observed and identified as a phase of the Al–Cu system ($a = 0.2998$ nm, CsCl type) by X-ray diffraction. The grain size in Fig. 1c is very small (about 10 μm) and a finely dispersed cobalt-rich phase identified by EPMA appears in the grain interiors. Even in specimens heated at 900 °C for 10 h, this phase did not increase in volume. The microstructures in Figs 1d to f show typical equiaxial grains.

Figs 2a to f shows the microstructures of alloys 1 to 6, respectively, aged at 400 °C for 300 min. In Fig. 2a the area fraction of nodules is about 80%. There are few nodules in Fig. 2b and with longer heating times (10^5 min), the area fraction of the nodules does not increase. The whole surface is covered by nodules, in Fig. 2c, whereas there is little nodule formation in Figs 2d and e. In Fig. 2f the nodules cover a large fraction of the surface.

As shown elsewhere [4], the phases appearing after ageing treatment are α_2 and β phase in all six specimens.

3.2. Electrical resistivity, hardness, and area fraction of nodules

Fig. 3 shows change in electric resistivity, hardness, and area fraction of nodules for alloys 1 to 6 aged at 300 °C. In Fig. 3a, ρ and ρ_0 are specific resistivities with solution treatment and ageing times. As it was impossible to cold work the alloy 2 by drawing, the electrical resistivity was not measured. The electrical resistivity curve for alloy 4 does not decrease as

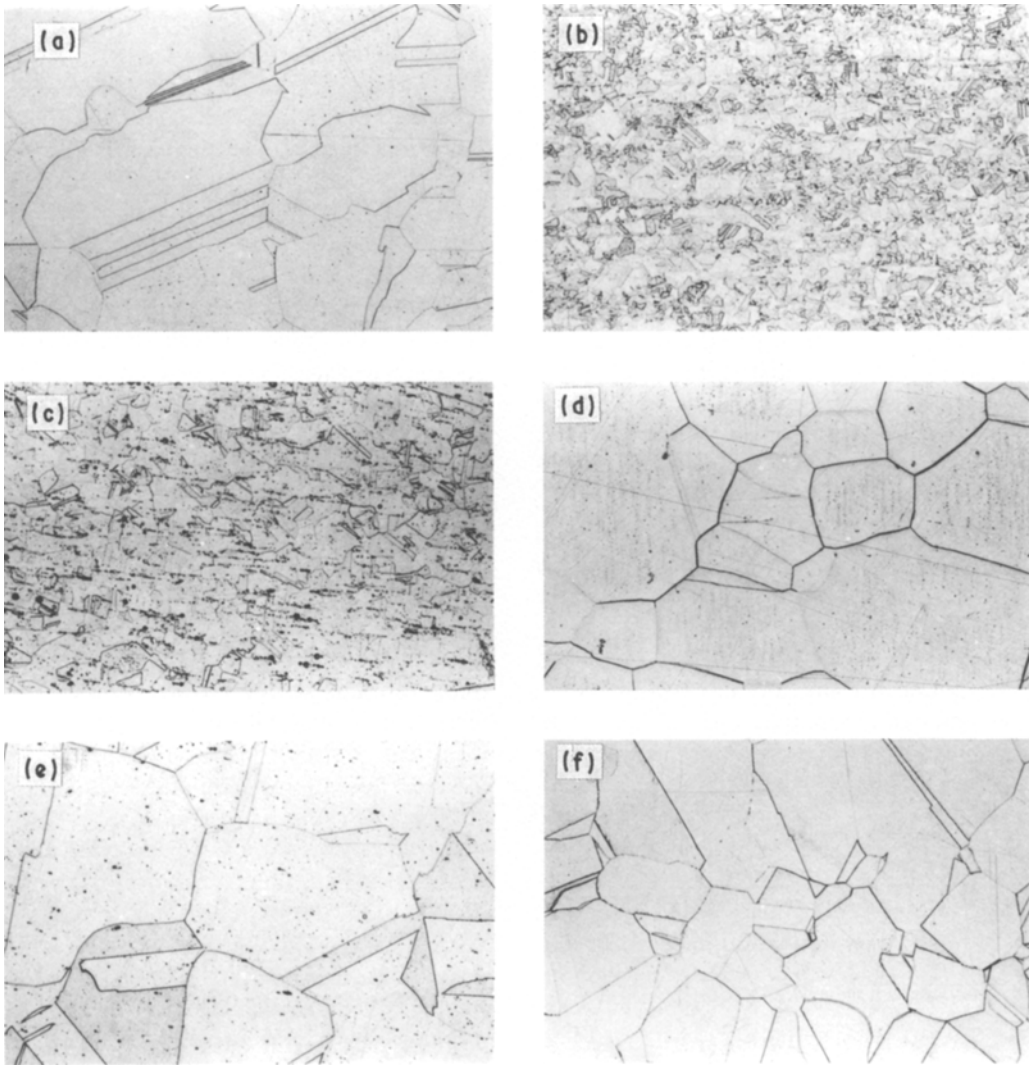

Figure 1 Microstructure of alloys 1 to 6 solution treated at 900 °C. Alloys: (a) 1, (b) 2, (c) 3, (d) 4, (e) 5, (f) 6.

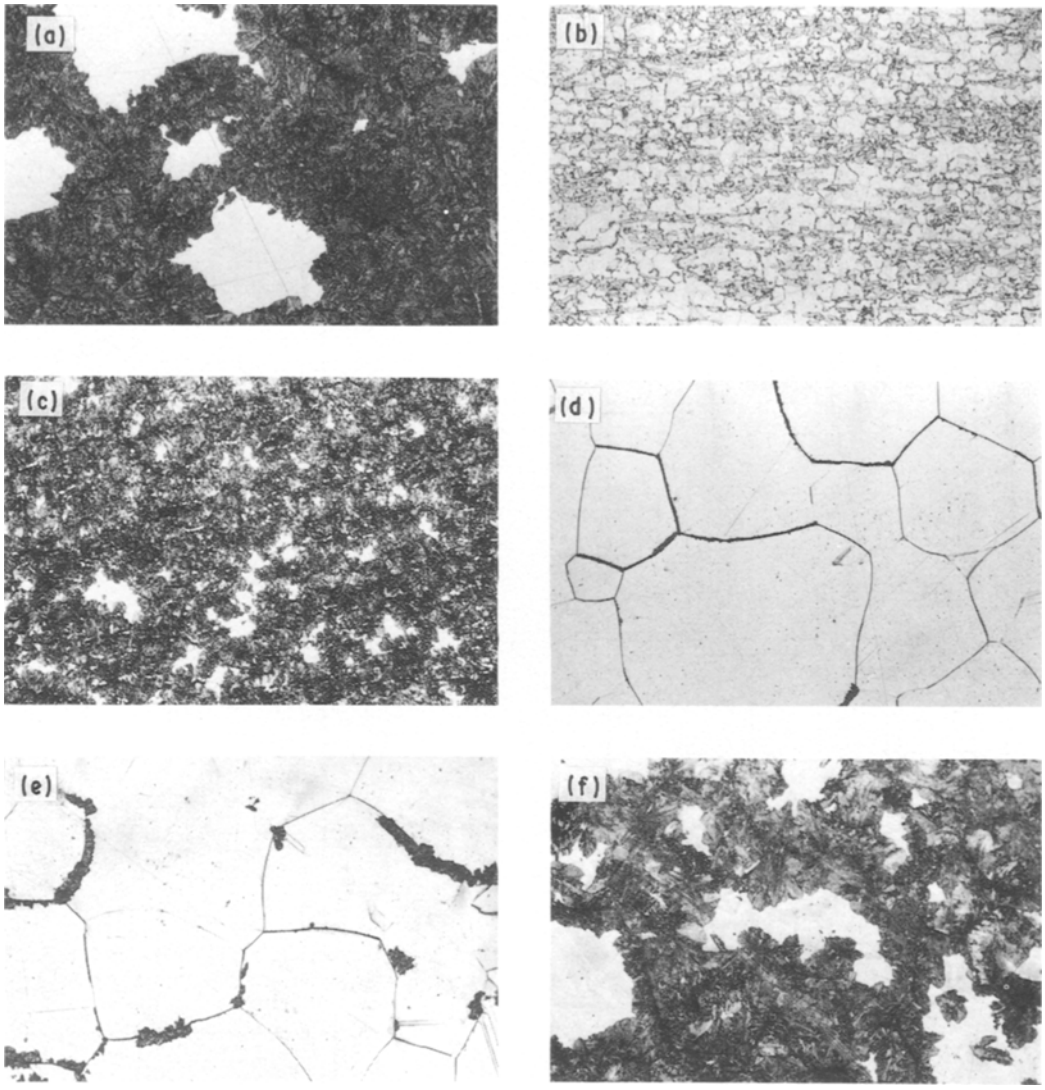

Figure 2 Microstructure of alloys 1 to 6 aged at 400 °C for 300 min. Alloys: (a) 1, (b) 2, (c) 3, (d) 4, (e) 5, (f) 6.

rapidly as the other alloys. With alloy 5, the electrical resistivity after ageing becomes higher than the values after solution treatment for the period investigated here.

In Fig. 3b, the dashed lines (marked Nd) show the nodule hardness. In alloy 2, these values are of the matrix area without intermetallic compounds of the Al–Cu systems. In alloy 3, the grain size is very small and Fig. 3 shows both matrix and nodule values. In the solid curves for alloys 2 and 3, where two phases exist after the solution treatment, hardening is slow and the maximum hardness of alloy 2 ($H_v = 220$) is lower than in alloy 1. The hardening process in alloys 4 to 6 is faster than in alloy 1. The addition of chromium (alloy 5) accelerates the grain interior precipitation most, and the hardness values in the matrix are high ($H_v = 172$) immediately after the solution treatment.

For Fig. 3c, the area fraction of nodules for alloys 2 and 3 could not be measured because these alloys do not become a single phase on the solution treatment. In alloy 1, nodule formation starts at 10^3 min and growth is rapid at 4×10^3 min, and finally the whole surface is covered with nodules. As previously reported [4], the electrical resistivity (Fig. 3a) decreases rapidly from the start of nodule formation in alloy 1.

Figs 4 and 5 show changes in electrical resistivity, hardness, and area fraction of nodules aged at 350 and 400 °C. The grain-boundary reaction on the addition of elements is decreasingly retarded with higher temperatures, and both tin and chromium show similar changes during nodule formation.

3.3. Retardation mechanism of grain-boundary reaction by small additions of elements

Fig. 6 shows the relation between the width of the nodule, W, and the ageing time at 400 °C. The slope shows the growth rate of the nodules: 0.25 μm min^{-1} for alloy 1; 0.014 μm min^{-1} for alloy 2; 0.02 μm min^{-1} for alloy 5; 0.20 μm min^{-1} for alloy 6; the growth rate with tin is 1/18 of the alloy without additions.

To determine the retardation mechanism of the nodule formation by the added elements, it is necessary to determine whether the elements act at the nucleation or the growth stage of the nodules. Cahn [5] suggested a relation to growth rate and grain size with the degree of saturation of the nucleus at the nucleation site in pearlite reactions. The degree of site saturation expresses how many nuclei exist at the

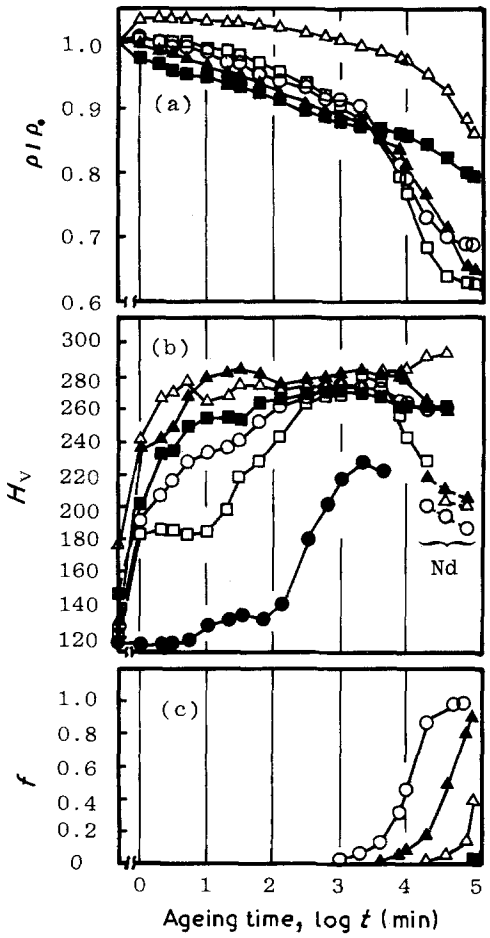

Figure 3 (a) Electrical resistivity, (b) hardness, and (c) area fraction of nodules, after ageing at 300 °C. Alloys: (○) 1, (●) 2, (□) 3, (■) 4, (△) 5, (▲) 6.

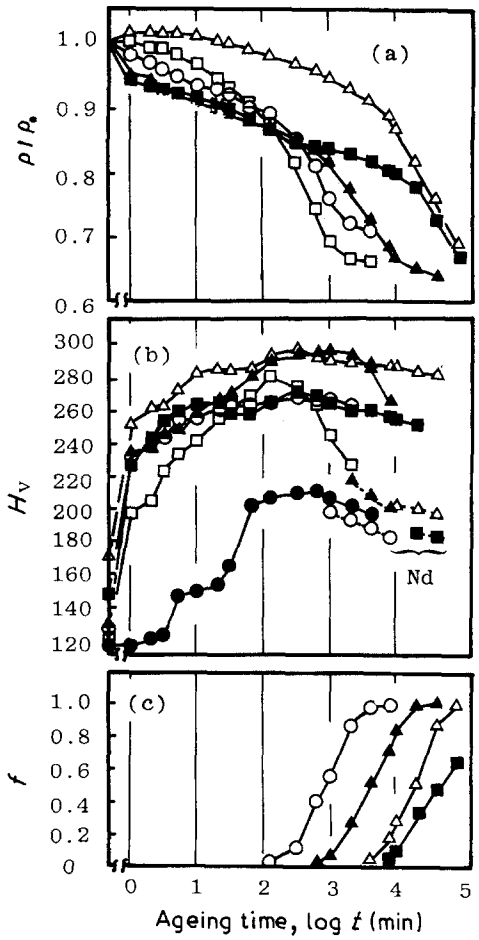

Figure 4 (a) Electrical resistivity, (b) hardness, and (c) area fraction of nodules, after ageing at 350 °C. For key, see Fig. 3.

nucleation site

$$0.1 < vt_{0.5}/d < 0.4 \quad (1)$$

where v is the growth rate of pearlite, $t_{0.5}$ is the time until half the alloy is transformed, and d is the grain size. When Equation 1 holds, sites for nucleation are saturated by nuclei early in the ageing process. Table II shows v, $t_{0.5}$, and d (= 120 μm) from Figs 1, 5c, and 6, showing that Equation 1 is satisfied for all the alloys at 400 °C. It may be assumed that nucleation sites are saturated by nuclei early in the ageing of these alloys. As a result the nucleation of nodules is easy and growth is retarded by the addition of elements.

Generally, there are three main mechanisms by which element additions retard grain-boundary reactions.

1. When the added element concentrates in only one of the nodule phases, and diffusion across the grain boundary is retarded [6].

2. When the added element segregates at the grain boundary, and nucleation of nodules or movement of the grain boundary is retarded [7].

3. Movement of the nodule interface is blocked by precipitates in the grain interior which have been stabilized by the added element [8].

With mechanism 1 the added element concentrates in the α_2 or β phase of the nodule, and is slightly soluble in intermetallic compounds and the ordered lattice. Both tin and indium are significantly soluble,

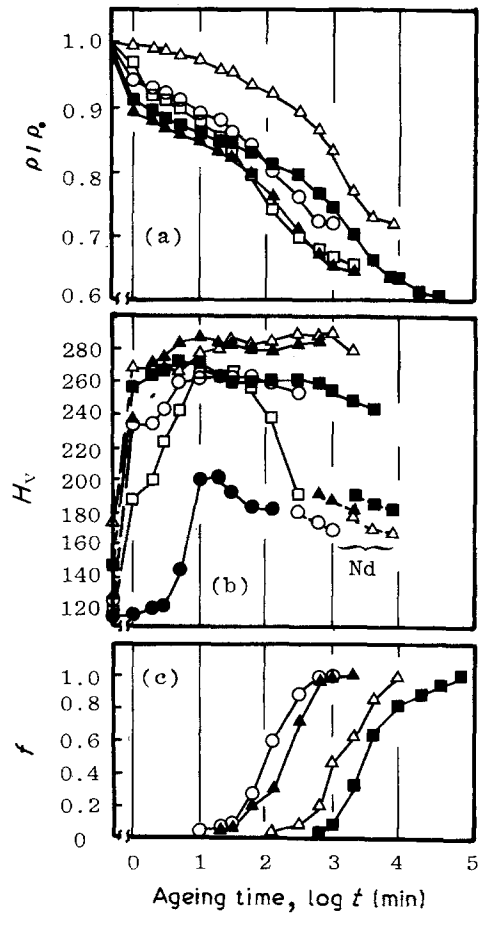

Figure 5 (a) Electrical resistivity, (b) hardness, and (c) area fraction of nodules, after ageing at 400 °C. For key, see Fig. 3.

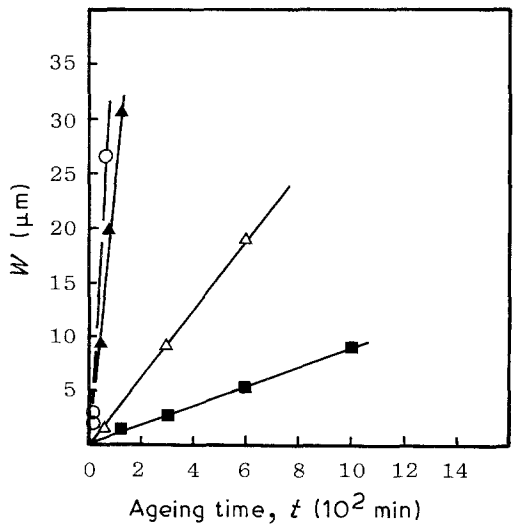

Figure 6 Nodule width, W plotted against ageing time at 400 °C. Alloys: (○) 1, (■) 4, (△) 5, (▲) 6.

TABLE II Growth velocities, v and the time for half the alloys to react ($t_{0.5}$)

Alloy	V	$t_{0.5}$	$Vt_{0.5}/d$
1	0.25	100	0.21
4	0.01	2900	0.24
5	0.02	1200	0.20
6	0.20	190	0.32

about 10 and 20 mass % in silver at 400 °C [9], and would have to concentrate in the phase only. As a result, the grain-boundary reaction is retarded, more with indium than with tin addition, because indium is more soluble in silver. However, as shown in Fig. 6, tin addition causes significant retardation and the effect of indium addition is not clear. Therefore, theory 1 does not explain the experimental results.

No segregation near the grain boundary was observed by EPMA in the solution-treated alloys. With cobalt (alloy 3) there may be segregation at the grain boundary after solution treatment, but the grain-boundary reaction is not retarded. Therefore, theory 2 does not explain the experimental results either.

With theory 3, retardation of nodule growth is explained as follows. Grain-interior reactions take place earlier than grain-boundary reactions in the alloys here, as X-ray diffraction patterns of α_2 and β phases are sharp, showing that there is no internodule strain and that the nodule hardness is lower than the grain interior. Therefore, it may be assumed that grain-boundary precipitates are not included in the nodules. As a result the two processes, grain-interior precipitate decomposition and diffusion, must take place prior to the grain-boundary reaction.

It is considered that tin is especially stable to grain-interior precipitates and that it retards their decomposition. As a result, the added elements decrease the mobility of the nodule interface. As stated previously, differences in melting points between the alloy and the added element were considered in selecting the elements for addition. As a result, it is concluded that mechanism 3 above, where the element forms stable grain-interior precipitates and effectively retards the grain-boundary reaction, is the grain-boundary reaction of the added elements.

3.4. Activation energy for grain-interior and grain-boundary reactions

Fig. 7 shows the relation between the ageing time when electrical resistivity changes 10% ($\rho/\rho_0 = 0.1$) and $1/T$. The slopes of this relation give the activation energy for the grain-interior reaction, before the nodular reaction takes place. The values are 192 to 196 kJ mol^{-1} and the differences between the added elements are small. Yasuda [10] and Ohta *et al.* [11] have reported that the products of grain-interior reactions were Guinier–Preston (G–P) zones and PdCu superlattices of the AuCu-11 type. Activation energies for diffusion in binary systems of copper and palladium in silver are 192 and 238 kJ mol^{-1}, respectively [12]. The alloys in the present work are quaternary systems, and it may seem inappropriate to make

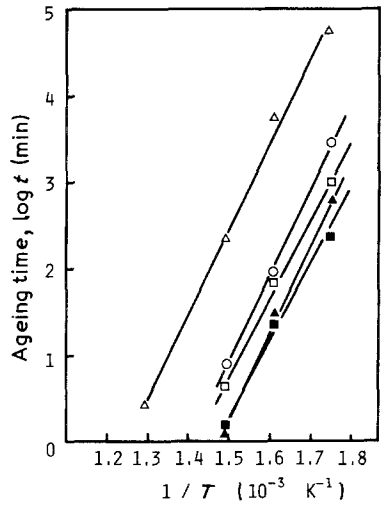

Figure 7 Arrhenius plots of ageing time for 10% electrical resistivity change (ρ/ρ_0). Alloys: (○) 1, (□) 3, (■) 4, (△) 5, (▲) 6.

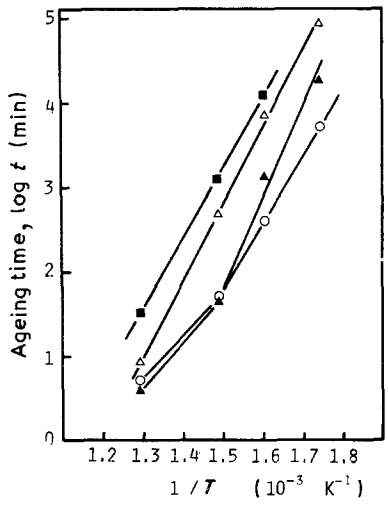

Figure 8 Arrhenius plots of ageing time at 15% area fraction of nodules ($f = 0.15$). For key, see Fig. 6.

comparisons with a binary system. However, the values are similar and may represent the activation energies for the diffusion of copper and palladium in silver.

Fig. 8 shows the relation between the ageing time when the area fraction of nodules reaches 15% ($f = 0.15$) and $1/T$. The resulting activation energies of nodule growth are 144 to 208 kJ mol^{-1} for the alloys in the 300 to 400 °C range. Generally, activation energy for grain-boundary diffusion is one-half to one-third of the activation energy for volume diffusion. The values here are rather large. If the rate of nodule growth is determined by grain-boundary diffusion, as reported for many alloy systems [13, 14]. Therefore, it is considered that the values here are related to the decomposition of the grain-interior precipitates.

4. Conclusion

The grain-boundary reactions in Ag–25 mass % Pd–10 mass % Cu alloys with 1 mass % additions of aluminium, cobalt, tin, chromium or indium, were investigated by optical microscopy, electrical resistivity, and hardness tests. The main results are as follows.

1. Additions of tin and chromium retarded grain-boundary reactions. The growth rate of nodules with tin added decreases to 1/18 of the non-added alloy.

2. Grain interior reactions are accelerated with chromium, tin and indium addition, with chromium being the most effective.

3. The activation energies for the grain-interior and grain-boundary reactions are 192 to 196 and 144 to 208 kJ/mol, respectively.

4. Additions retard the growth but not the nucleation at the grain boundary.

Acknowledgement

This study was supported by a Grant-in-Aid for Scientific Research 1986 (A-61771605) from the Ministry of Education, Science and Culture, Japan.

References

1. M. OHTA, K. HISATSUNE and M. YAMANE, *J. Jpn Soc. Dent. Appar. Mater.* **16** (1975) 87.
2. H. ISAKA, *ibid.* **28** (1977) 137.
3. S. TANAKA, *ibid.* **21** (1980) 263.
4. I. KAWASHIMA, Y. KANZAWA, Y. ARAKI and H. OHNO, *J. Jpn Inst. Metals* **53** (1989) 14.
5. J. W. CAHN, *Acta Metall.* **4** (1956) 449.
6. J. W. CAHN, *Trans. AIME* **209** (1957) 140.
7. M. MIKI and Y. OGINO, *J. Jpn Inst. Metals* **48** (1984) 347.
8. M. MIKI, T. KITAYAMA and Y. AMANO, *ibid.* **44** (1980) 170.
9. M. HANSEN, "Constitution of Binary Alloys", 2nd Edn (McGraw-Hill, New York, 1958) p. 52.
10. K. YASUDA, *J. Jpn Soc. Dent. Appar. Mater.* **10** (1969) 156.
11. M. OHTA, T. SHIRAISHI, K. HISATSUNE and M. YAMANE, *J Less-Common Metals* **59** (1980) 1966.
12. Japan Institute of Metals, "Kinzoku data book", 2nd Edn (Maruzen, Tokyo, 1984) p. 24.
13. K. RUSSEW and W. GUST, *Z. Metallkde* **70** (1979) 522.
14. S. P. GUPTA, *ibid.* **77** (1986) 472.

Received 26 February
and accepted 9 March 1990